

Route to three-dimensional fragments using diversity-oriented synthesis

Alvin W. Hung^a, Alex Ramek^b, Yikai Wang^b, Taner Kaya^a, J. Anthony Wilson^a, Paul A. Clemons^a, and Damian W. Young^{a,1}

^aChemical Biology Program, Broad Institute of Harvard and Massachusetts Institute of Technology, 7 Cambridge Center, Cambridge, MA 02142; and ^bDepartment of Chemistry and Chemical Biology, Harvard University, 12 Oxford Street, Cambridge, MA 02138

Edited by Stuart L. Schreiber, Broad Institute, Cambridge, MA, and approved March 3, 2011 (received for review December 22, 2010)

Fragment-based drug discovery (FBDD) has proven to be an effective means of producing high-quality chemical ligands as starting points for drug-discovery pursuits. The increasing number of clinical candidate drugs developed using FBDD approaches is a testament of the efficacy of this approach. The success of fragment-based methods is highly dependent on the identity of the fragment library used for screening. The vast majority of FBDD has centered on the use of *sp*²-rich aromatic compounds. An expanded set of fragments that possess more 3D character would provide access to a larger chemical space of fragments than those currently used. Diversity-oriented synthesis (DOS) aims to efficiently generate a set of molecules diverse in skeletal and stereochemical properties. Molecules derived from DOS have also displayed significant success in the modulation of function of various “difficult” targets. Herein, we describe the application of DOS toward the construction of a unique set of fragments containing highly *sp*³-rich skeletons for fragment-based screening. Using cheminformatic analysis, we quantified the shapes and physical properties of the new 3D fragments and compared them with a database containing known fragment-like molecules.

library development | probe discovery

The elucidation of small-molecule probes that shed light on fundamental and disease-associated biological phenomena is a powerful approach in modern chemical biology (1, 2). The predominant mechanism through which such probes are discovered today is the high-throughput screening (HTS) of various small-molecule screening collections (3). Success at the approach is inextricably linked to the identity and the quality of the screening collection. Synthetic organic chemistry has played a pivotal role in generating large collections of small molecules to be screened in various HTS campaigns. However, much work remains to be done toward the generation of the optimal screening collection (4). Clearly, sources of chemicals with greater diversity are needed and alternative approaches toward probe development are warranted (5).

Fragment-based drug discovery (FBDD) is a complementary strategy to HTS and is a well-validated approach toward generating small-molecule leads (5, 6). Although the method has primarily been explored on targets of therapeutic relevance, it is reasonable to conceive that this method can also be applied to the production of probe molecules against an expanded array of biological targets. The central theme underlying FBDD is the screening of a library of low molecular weight compounds (<300 g/mol) (7), or “fragments,” against a specific biological target. The small size of fragments enhances the probability of complementary binding. Moreover, it has also been argued that fragment space is substantially smaller than nonfragment space such that orders of magnitude fewer molecules within a screening library are needed relative to HTS to achieve “hits” (7, 8). However, unlike HTS where hits are generally more potent (nanomolar to low micromolar), the binding interactions of fragments tend to be considerably weaker (micromolar to millimolar); consequently, they require very sensitive biophysical techniques

capable of picking up such weak interactions (9). After an appropriate fragment hit has been identified, it then serves as a constructive chemical anchor for the generation of a ligand with much greater potency, which is achieved synthetically by “growing” or “linking” fragments (10). These strategies are most efficiently executed when an X-ray or NMR structure of the target is available giving critical binding information (11). In this vein, follow-up chemistry is guided in a rational manner requiring fewer analogs to be made toward a potent lead compound.

Nature recognizes small molecules in a complementary 3D fashion (12). Therefore, a fragment library designed with the intention of generating compounds with high molecular shape diversity would be expected to display a broader range of biological activities. The increasing numbers of commercial vendors selling fragments have certainly been a boon to the advancement of fragment-based drug discovery. However, most fragment libraries used to date have been limited to aromatic heterocycles with an underrepresentation of chiral *sp*³-rich compounds (13). The growing and linking approaches applied to some of these simple planar *sp*²-rich fragments have undoubtedly led to the generation of unique and high-potency lead compounds (6, 14, 15). Nonetheless, restricting fragment screening to the use of only *sp*³-deficient planar molecules inherently limits exploration to a smaller subset of biological spaces. In contrast, the use of more complex and *sp*³-rich (more 3D-like) fragments would certainly increase the fragment chemical space, which might in turn be advantageous in exploring more demanding biological targets. To date, there has been little discussion in the literature toward the synthetic preparation of chemically diverse fragments libraries.

Given the above discussion, we initiated a research program aimed at creating 3D fragments to be used in a fragment-based approach to discover alternative small-molecule probes. To accomplish this goal, we turned to diversity-oriented synthesis (DOS) (16, 17), an important guiding principle for the generation of small molecules with disparate properties for biological interrogation. Although DOS has proven successful in producing molecules used in HTS (18, 19), to the best of our knowledge, the concept has not explicitly been applied toward the generation of low molecular weight fragments. Through DOS, short and efficient synthetic pathways are constructed, giving rise to small molecules with diverse shapes and physical properties. Recently, the build/couple/pair (B/C/P) algorithm has emerged as an efficient DOS approach to synthesize structurally and stereochemically diverse compounds (20, 21). The “build” phase encompasses obtaining stereochemically diverse starting materials. It is most desirable to obtain chiral building blocks in all possible

Author contributions: A.W.H. and D.W.Y. designed research; A.W.H., A.R., Y.W., T.K., J.A.W., and P.A.C. performed research; A.W.H., A.R., Y.W., T.K., J.A.W., and P.A.C. analyzed data; and A.W.H. and D.W.Y. wrote the paper.

The authors declare no conflict of interest.

This article is a PNAS Direct Submission.

¹To whom correspondence should be addressed. E-mail: dyoung@broadinstitute.org.

This article contains supporting information online at www.pnas.org/lookup/suppl/doi:10.1073/pnas.1015271108/-DCSupplemental.

stereoisomeric combinations. In the “couple” phase, these building blocks are unified, usually in a matrix fashion leading to all possible stereoisomeric combinations of a higher-ordered structure. Finally, in the “pair” phase, the structures created in the couple phase are subjected to various reaction conditions to effect intramolecular reactions leading to rigidified and more complex structures.

We decided that the construction of nonaromatic, high- sp^3 content, and chiral fragments would be appropriate to test our hypothesis concerning the relevance of diverse 3D fragments. To these ends, a B/C/P strategy was devised that would provide quick access to small fused bicyclic and spirocyclic fragments. The pathways were constructed to generate small molecules adhering to the “fragment rule of three” (22), confining them to a molecular weight of less than 300 g/mol, a maximum of three hydrogen-bond donors/acceptors, and a maximum of three rotatable bonds. The generation of such fragments would enable us to examine the validity of such structures within a fragment discovery-based paradigm.

Results

The build phase of our pathway started with selection of proline building blocks **1–3** (Fig. 1). One factor for selecting these compounds was the readily available enantiomerically pure versions of both D and L amino acids. The use of different stereoisomers as starting building blocks for synthesis allows for the generation of a stereochemically diverse set of fragments. Additional benefits of using proline building blocks include the extensive amount of chemistry focusing on the generation of pyrrolidine-based scaffolds. This information is constructive given that, if binders are found, numerous substituted pyrrolidines can be generated in the follow-up chemistry phase from a variety of known methods (23).

Proline derivatives **1** and **2** were synthesized and isolated using modified synthetic procedures proposed by Harris et al. (24) (*SI Appendix, Scheme S1*). The vinyl functional groups installed in proline **1** and **2** were seen useful for subsequent pairing reactions to form bicyclic fragments. Building block **3**, on the other hand, was generated by employing Seebach's concept of self-reproduction of chirality (25), which was reinvestigated by Wang and Germanas (26) (*SI Appendix, Scheme S2*). This compound was chosen as a starting building block because of its enantiomerically pure quaternary carbon center that would enable access to spirobicyclic compounds. Furthermore, both antipodes of **3** can also be obtained using the methodology of Seebach (25).

With compounds **1–3** in hand, we proceeded to the couple and pair phases of our pathway. Figs. 2 and 3 illustrate two examples of the implementation of this strategy. Intermolecular coupling reactions based around building blocks **1** and **3/3'** yielded more densely functionalized pyrrolidine molecules (compounds **4a–14a**) (24, 27, 28), which when paired under various conditions afforded skeletally diverse bicyclic fragments of varying ring sizes. Besides possessing distinctive fragment scaffolds, these assembled bicyclic compounds were also diverse with respect to stereochemistry. It is noteworthy that the stereogenicity of the

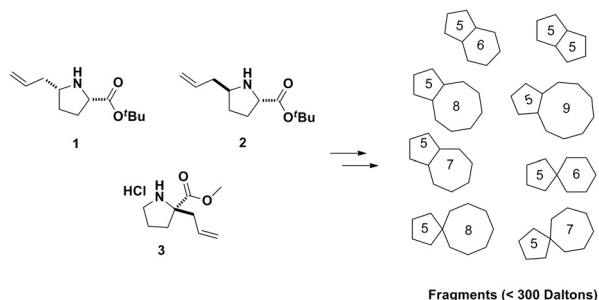


Fig. 1. Building blocks **1**, **2**, and **3** were synthesized for the preparation of a 3D fragment library.

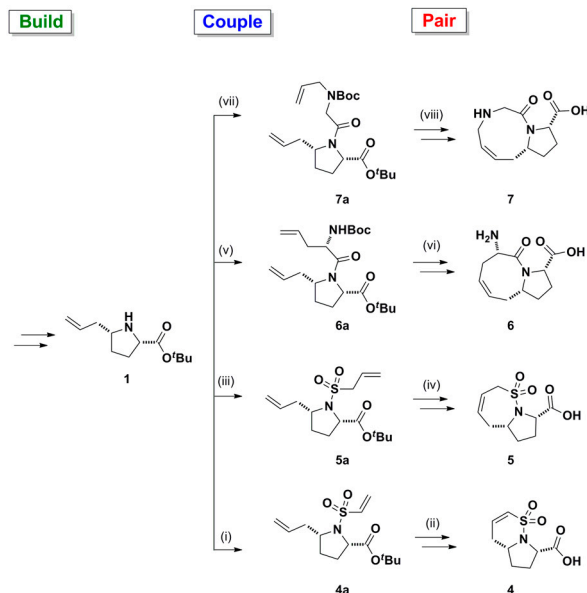


Fig. 2. Application of a B/C/P approach starting from proline **1** yielding bicyclic compounds **4–7**: (i) 2-chloroethanesulfonyl chloride, Et_3N , CH_2Cl_2 , 46%; (ii) Grubbs II, CH_2Cl_2 , reflux, 80%; TFA; (iii) prop-2-ene-1-sulfonyl chloride, Et_3N , CH_2Cl_2 , 48%; (iv) Grubbs II, CH_2Cl_2 , reflux, 90%; TFA; (v) (S)-N-Boc-allylglycine, 1-ethyl-3-(3-dimethylaminopropyl) carbodiimide (EDCI), Oxyma, Et_3N , CH_2Cl_2 , 98%; (vi) Grubbs I, CH_2Cl_2 , reflux, 87%; TFA; (vii) N-Boc-N-allylglycine, EDCI, Oxyma, Et_3N , CH_2Cl_2 , 97%; (viii) Grubbs I, CH_2Cl_2 , reflux, 60%; TFA.

final fragments arises from the build and couple phases, whereas the skeletal diversity is achieved predominately in the pairing phase.

In the coupling phase, compounds **6a–9a** and **14a** were synthesized using 1-ethyl-3-(3-dimethylaminopropyl)-carbodiimide-mediated coupling methods with commercially available olefin-containing compounds. The use of established peptide synthesis methods, and addition of ethyl(hydroxyimino)cianoacetate (Oxyma) (29) as an additive to the carbodiimide-mediated amide bond formation, reduces racemization, allowing for stereochemical control in the coupling reactions. Finally, in the pairing phase, the ruthenium-catalyzed ring-closing metathesis (RCM) reactions yielded compounds **6–9** and **14**.

Coupling of proline derivatives **1** and **3** with 2-chloroethanesulfonyl chloride or prop-2-ene-1-sulfonyl chloride in the presence of a base afforded vinyl sulfonamides **4a**, **5a**, **11a**, and **12a** (30). Subsequent RCM on the coupled sulfonamides gave the desired **5-6** and **5-7** sultam rings in high yields. The facile sulfonylation pairing reactions used in tandem with efficient RCM pairing reactions enables bicyclic compounds **4**, **5**, **11**, and **12** to be rapidly synthesized (three steps). Fragment **13** was synthesized according to procedures described by Zhou and Hanson (30). Reduction of proline **3** gave the corresponding pyrrolidine alcohol which upon protection using *tert*-butyl dimethyl silyl (TBS) chloride yielded compound **13b** (*SI Appendix*). The TBS-protected pyrrolidine **13b** was then coupled with 2-chloroethanesulfonyl chloride in the presence of triethylamine to give **13a**. Removal of the TBS-protecting group allowed for an intramolecular oxo-Michael pairing reaction affording fragment **13**.

In an effort to generate spirocyclic fragments, commercially available starting material **3'** (derivative of compound **3**) was coupled with allylamine (Scheme 1). The RCM of **9a'** failed to generate the cyclized product because the thermodynamically favored rotamer of the secondary amide causes the two allyl groups to be poised away from each other. To overcome this problem, **9a'** was methylated yielding the tertiary amide **9a**, which

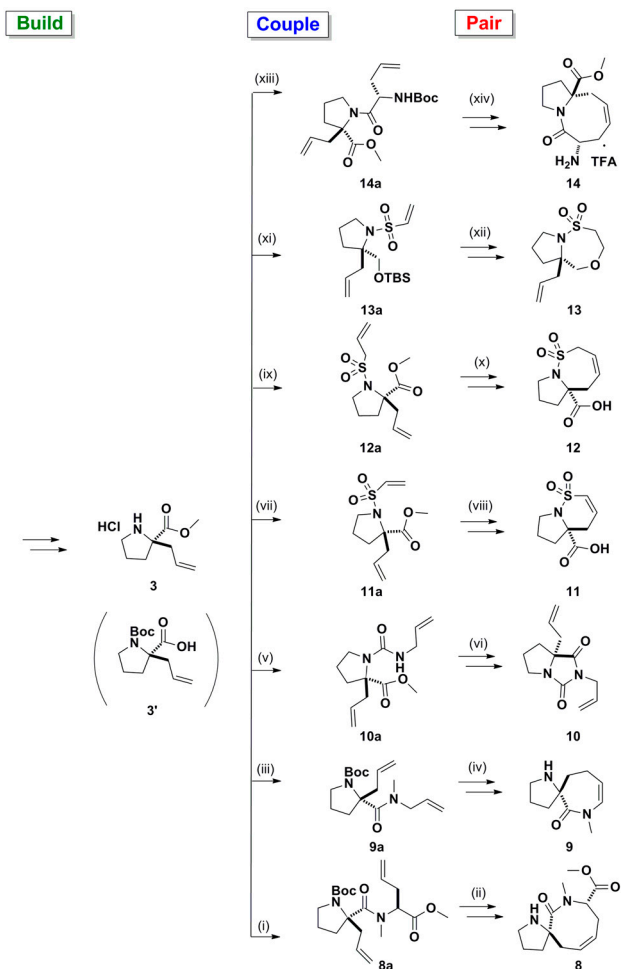
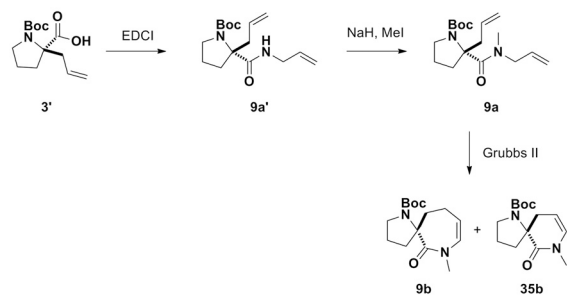


Fig. 3. Application of a B/C/P approach starting from proline 3/3' to give compounds 8–14. From 3', (i) (S)-allylglycine methyl ester, 1-ethyl-3-(3-dimethylaminopropyl) carbodiimide (EDCI), Oxyma, Et₃N, CH₂Cl₂, 89%; NaH, MeI, DMF, 89%; (ii) Grubbs II, CH₂Cl₂, reflux, 34%; TFA; (iii) allylamine, EDCI, Oxyma, Et₃N, CH₂Cl₂, 91%; NaH, MeI, dimethylformamide (DMF), 72%; (iv) Grubbs II, toluene, 60%; TFA. From 3, (v) allyl isocyanate, Et₃N, CH₂Cl₂, 70%; (vi) NaH, DMF, 93%; (vii) 2-chlorosulfonyl chloride, Et₃N, CH₂Cl₂, 62%; (viii) Grubbs II, CH₂Cl₂, reflux, 92%; LiOH, THF, 53%; (ix) prop-2-ene-1-sulfonyl chloride, Et₃N, CH₂Cl₂, 44%; (x) Grubbs II, CH₂Cl₂, reflux, 96%; LiOH, THF, 71%; (xi) LiAlH₄, THF; *tert*-butyldimethylsilylchloride, Et₃N, CH₂Cl₂ (24% over two steps); 2-chlorosulfonyl chloride, Et₃N, CH₂Cl₂, 33%; (xii) tetrabutylammonium fluoride, THF, 45%; (xiii) (S)-N-Boc-allylglycine, EDCI, Oxyma, Et₃N, CH₂Cl₂, 48%; (xiv) Grubbs II, CH₂Cl₂, reflux, 41%; TFA.

allowed for the two rotamers to be isothermic and interconvertible. The subsequent RCM of **9a** gave rise to two enamides, a major product **9b** and a minor product **35b**. In both products, migration of the double bond was observed, which is indicative of isomerization during the RCM reaction, presumably catalyzed by ruthenium hydride species (31, 32). Formation of the six-membered enamide **35b** can be rationalized on grounds that the migration of the double bond occurred before the RCM releasing propene (instead of ethylene) to generate **35b**. However, migration of the double bond in situ was not observed in the RCM of tertiary amide **8a** and the desired spirocyclic product **8b** was obtained (see *SI Appendix*).

In total, a complete matrix of diastereomers of unsaturated and saturated forms of 5-6, 5-7, 5-8, and 5-9 bicyclic fragments was achieved by iterative coupling of different stereoisomeric building blocks. The mixing and matching of various stereogenic building blocks followed by versatile RCM pairing reactions generated a complete set of all possible diastereomers (Fig. 4).



Scheme 1. Synthesis of spirocyclic enamide **9b** and **35b** from building block **3'**.

The devised B/C/P strategy not only created a small library of fragments of diverse skeletal structures, but also one rich in stereochemical variation.

The availability of all diastereomeric configurations of these fragments is valuable and enables systematic evaluation of the stereochemical and structural relationships between different fragments binding against various biological targets. Stereochemical relationships are especially important in the case of fragments where the size limit and complexity of the molecules can produce very stringent structure–activity relationships. The difference between the various stereoisomers might be significantly large enough to completely obliterate binding. The insights obtained from the stereochemical modifications between the fragments would then support better design of a more potent inhibitor. We envisioned applying the same chemistry to D-proline so as to produce all the enantiomeric forms of the compounds, allowing for our library to cover a greater chemical space, ultimately enabling for the probing of a wider biological space.

In addition to structural and stereochemical diversity, we designed a third diversity element into our library: a “postpairing phase.” Fragments, because of their low molecular weight usually display weak binding affinities. Consequently, the particular functional groups within a given fragment are critical to the observation of a binding event. Subtle changes in functionalities and shape of fragments can result in significant changes to binding affinities. Accordingly, we determined that it would be imperative to take the scaffolds that were assembled in the B/C/P strategy and perform functional group interconversion reactions on them to produce new fragments. The result of these modifications would be to generate “functional group diversity” within the fragment library. Methyl esters in compounds **11b**, **12b** (*SI Appendix*), and **14** were hydrolyzed to the carboxylic acids to give fragments **11**, **12**, and **14c** (*SI Appendix*). These functional interconversions would have a significant impact on the overall electronic properties of the fragments. The reduction of olefins in the fragments was also performed (Fig. 5), resulting in increased *sp*³ carbon atom content and a different conformational profile for the reduced fragments.

Discussion

There have been several recent studies demonstrating the benefits of increasing the saturation content in drug-like compounds (33). Potential oral drug candidates with fewer aromatic rings were found to be more “developable” and drug-like than the ones with more aromatic rings (34). Also, the increased *sp*² content of a molecule was found to negatively correlate with the aqueous solubility of the compound (34), suggesting the possibility of improving clinical success with increasing the saturation content of drug candidate. Other studies that have focused on the binding of diverse small molecules by using small-molecule microarrays quantitatively found that molecules containing more *sp*³-hybridized and stereogenic atoms have improved binding selectivity and frequency toward a set of 100 proteins (35). The importance of *sp*³-rich lead compounds in these studies can be easily

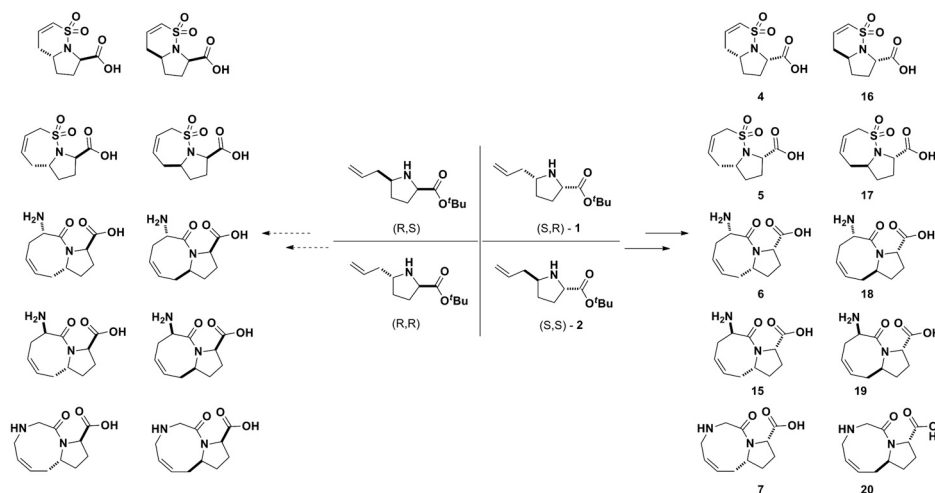


Fig. 4. Using a B/C/P approach to obtain the full matrix of all possible diastereomeric products.

extended to the molecular makeup of fragments. Taken together, these investigations reinforce our hypothesis about the advantages of building a fragment library populated with more sp^3 -rich molecules.

The design of diverse fragments based on the inclusion of more sp^3 carbon atoms should result in the ability of such fragments to bind to distinct sites on biological targets relative to flat and achiral ones. Doing so could potentially provide many opportunities to develop leads in probe or drug-discovery campaigns. Equally important, increasing the saturation also provides for unique and different geometric “growth vectors” off of a fragment. This situation enables orientation-dependent growth and extension of fragments into pockets of an active site that might otherwise be inaccessible to planar aromatic fragments. Generation of more sp^3 -rich and chiral fragments would also mean greater access to different stereoisomers of the compounds. Such a strategy may enrich a fragment library collection and allow for powerful stereochemical structure–activity relationships when fragments are tested against various targets.

In addition to shape, fragments should also possess desirable physical properties for screening and facilitate follow-up chemistry. Chemical functional handles such as carboxylic acids and amine groups were deliberately incorporated in the final fragment products. These polar groups greatly enhance the solubility of the fragments, allowing them to be screened at higher concen-

trations under aqueous conditions. Additionally, these functional groups will also serve as hydrogen-bonding donors and acceptors, improving binding potency against target biological macromolecules. Finally, the presence of such functional groups was anticipated to promote the facile elaboration or modifications of fragments (fragment growing and linking) into probe or lead drug-like compounds.

Regarding the synthetic route, the application of the B/C/P pathway allowed for coupling of different substrates onto similar building blocks **1** and **3**, which made possible the construction of an array of bicyclic and spirocyclic fragments varying in molecular architectures (Figs. 2 and 3). This process is further amenable to a wider variety of other different coupling partners, allowing for rapid construction of varied fragments for library production. An additional advantage of the B/C/P approach in DOS is that it is highly modular. Because there is a high degree of control on each position of the building blocks and coupling partners, there is an ability to grow or link fragments at more positions on the fragment template. A mode of synthesis such as this provides an unparalleled access to derivatives from initial hits without changing the overall synthetic pathway.

To provide a more rigorous analysis of the synthesized fragment library, we applied computational methods to capture and quantify information about structural differences between the new fragment library (*SI Appendix*, Fig. S1) and a representative set of fragments obtained from the ZINC database (36, 37). A visual inspection of the principal moment-of-inertia (PMI) (38) plot (Fig. 6A) revealed more uniform coverage of molecular shapes for 35 of the synthesized 3D fragments as opposed to 18,534 more “conventional” fragments obtained from the ZINC database. To test this hypothesis, we triangulated the points within PMI space for the fragment library and calculated the areas of each triangle. We median-centered the areas, binned the compounds to a histogram, normalized, and performed a one-sided Kolmogorov-Smirnov (KS) test to evaluate whether the fragment library had a more uniform variance compared to the ZINC library. Results confirmed that the ZINC library was less uniform ($p = 7.14 \times 10^{-06}$). Further visualization of the PMI space of all the compounds obtained from the ZINC database (gray) shows most compounds skewing toward the left edge of the PMI space, indicative of structures possessing mainly rod-like or disc-like geometric features. Conversely, the 3D fragments (red) appeared to be more evenly spread out within the PMI plots, with none possessing entirely rod-like or disc-like (flat) features. This observation was confirmed by calculating a KS test between distances to the flat ($p = 1.25 \times 10^{-3}$) and rod-like ($p = 1.25 \times 10^{-3}$) corners for the ZINC fragments and the fragment library. However,

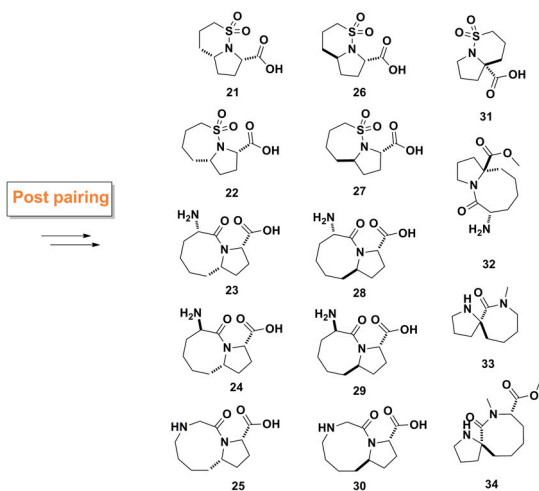


Fig. 5. Reducing the olefin groups in a postpairing phase to generate a new set of fragments.

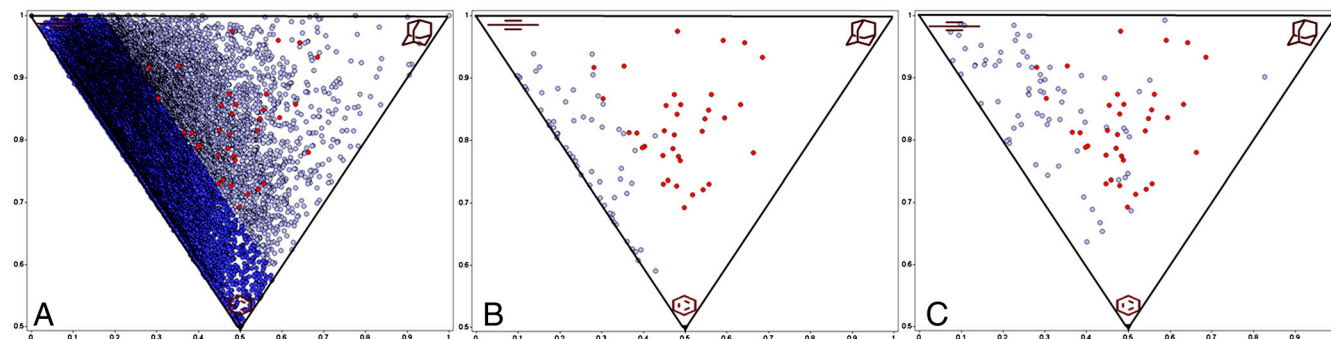


Fig. 6. Molecular shape analysis. Each corner on the triangular PMI plot indicates compounds with certain shape characteristics. The top left-hand corner of the PMI represents compounds with rod-like features (e.g., acetylene), the top right corner represents compounds with spherical features (e.g., adamantane), and the bottom corner represents compounds with disc-like features (e.g., benzene). (A) PMI plot depicting 35 3D fragments from this study (red) and 18,534 fragments obtained from ZINC database (gray). The darker-blue region represents 75% of the 18,534 fragments. (B) PMI plot depicting 35 3D fragments and 62 best-matched fragments from ZINC (gray), based on heavy atom count similarity. (C) PMI plot depicting 35 3D fragments and 76 of best-matched fragments from ZINC based on physicochemical descriptors.

results were not significant for distances to the sphere corner ($p = 0.14$), demonstrating even coverage of the newly synthesized 3D fragments, with no clustering of the fragments seen in the PMI space.

More striking is the comparison between the new fragment library and their best-matched fragment counterparts from ZINC. Two subsets of fragments were picked from within the ZINC fragment library to extend the comparison to a smaller number of related structures. First, we considered fragments that shared the same molecular formula (based on numbers of C, N, O, S), and second, we considered fragments that best matched our compounds using common physicochemical descriptors (molecular weight, calculated partition coefficient, number of hydrogen-bond donors and acceptors, number of rotational bonds, and polar surface area). In the first example, according to a KS test, the two different sets of fragments are significantly different in terms of distances to canonical PMI shapes (Fig. 6B; sphere, $p = 2.06 \times 10^{-21}$; disk, $p = 2.26 \times 10^{-11}$; rod, $p = 5.77 \times 10^{-7}$). Although possessing the same heavy atom chemical formula makeup, 62 of the best-matched fragments from the ZINC database were mainly planar and aromatic compounds, occupying the left boundary of the PMI plot. By comparison, the 3D fragments were more evenly distributed and tending toward the spherical corner of the plot. This difference in shape could be attributed to the effect of greater sp^3 content (as compared to flat aromatic compounds) of the designed fragment library. In the second example, we compared shapes of compounds that possessed similar physicochemical properties within ZINC to our fragments. The PMI analysis (Fig. 6C) showed the 3D fragment set to be distinctive relative to the closest matched fragments from ZINC. The shape distribution of the ZINC subset was once again residing toward left or sp^2 -rich edge of the triangle (sphere, $p = 2.06 \times 10^{-21}$; disk, $p = 4.03 \times 10^{-13}$; rod, $p = 1.53 \times 10^{-5}$). We infer from these results that, although physical properties of known fragment-type compounds are comparable to ours, their shapes tend to be mutually exclusive to one another.

Finally, in addition to shape analysis, a direct comparison was made between the calculated physical properties of the 3D fragments and the 18,534 compounds in ZINC (SI Appendix, Fig. S2).

As purposely intended from the DOS pathway design, the $sp^3/(sp^2 + sp^3)$ ratios for the 3D fragments were dramatically different than the ZINC fragments. On the other hand, the molecular weight, polar surface area, and logP values for the synthesized fragments all fell within the desired range of known fragments.

Conclusions

In summary, we have described the preparation of a series of diverse small molecules to be deployed in a fragment-based discovery approach using diversity-oriented synthesis. The molecules synthesized were derived from a B/C/P approach that gave access to diverse bicyclic and spirocyclic fragments while still keeping the size of the compounds down (<300 Da). Complexities of these fragments have been increased without the expense of increasing ligand size and weight. Cheminformatic analysis quantitatively confirmed that the goals of the intended synthesis were achieved and further validated that the properties of the library described will be amenable to a fragment-based screening approach.

DOS and fragment-based discovery have previously been viewed as unrelated activities (13). The merging of the two areas should combine the benefits offered from each approach and in doing so provide enhanced opportunities to deliver small molecules against valuable biological targets.

Materials and Methods

Synthetic schemes for building blocks 1–3 are given in the SI Appendix. A figure giving all the structures synthesized in this study is also included. Detailed experimental procedures describing the synthesis are included in the SI Appendix. All compounds were fully characterized by ^1H NMR, ^{13}C NMR (recorded at 500 MHz using a Variant I-500 instrument), and high-resolution mass spectrometry. Details about the computational analysis of the fragments are also discussed in the SI Appendix.

ACKNOWLEDGMENTS. The Center of Excellence in Chemical Methodology and Library Development (sponsored by National Institute of General Medical Sciences) enabled this research (Broad Institute Chemical Methodologies and Library Development, P50 GM069721). A.W.H.'s Fellowship is supported by Agency for Science Technology and Research Singapore.

- Schreiber SL (2009) Organic chemistry: Molecular diversity by design. *Nature* 457:153–154.
- Schreiber SL (2005) Small molecules: The missing link in the central dogma. *Nat Chem Biol* 1:64–66.
- Stockwell BR (2004) Exploring biology with small organic molecules. *Nature* 432:846–854.
- Payne DJ, Gwynn MN, Holmes DJ, Pompliano DL (2007) Drugs for bad bugs: Confronting the challenges of antibacterial discovery. *Nat Rev Drug Discov* 6:29–40.
- Congreve M, Chessari G, Tisi D, Woodhead AJ (2008) Recent developments in fragment-based drug discovery. *J Med Chem* 51:3661–3680.
- Murray CW, Rees DC (2009) The rise of fragment-based drug discovery. *Nat Chem* 1:187–192.
- Chessari G, Woodhead AJ (2009) From fragment to clinical candidate—a historical perspective. *Drug Discov Today* 14:668–675.
- Fink T, Raymond J-L (2007) Virtual exploration of the chemical universe up to 11 atoms of C, N, O, F: Assembly of 26.4 million structures (110.9 million stereoisomers) and analysis for new ring systems, stereochemistry, physicochemical properties, compound classes, and drug discovery. *J Chem Inf Model* 47:342–353.
- Ciulli A, Abell C (2007) Fragment-based approaches to enzyme inhibition. *Curr Opin Biotechnol* 18:489–496.

